Bulletin of the Seismological Society of America, Vol. 101, No. 1, pp. 399–403, February 2011, doi: 10.1785/0120100175

Short Note

Seismological Identification and Characterization of a Large Hurricane

by Carl W. Ebeling and Seth Stein

Abstract Much debate within the weather, climate, disaster mitigation, and insurance communities centers on whether rising sea-surface temperatures in the North Atlantic Ocean due to anthropogenic global warming are resulting in discernible trends in hurricane frequency or energy. However, some of the apparent increase in hurricane frequency may be due to the recent availability of aircraft- and satellite-based observations. A possible approach to this issue is via microseisms, seismic signals traditionally thought of as noise because they are not generated by earthquakes. These surface waves generated by ocean storms are detected even in continental interiors far from source regions. Here we show that the August 1992 Saffir/Simpson category 5 Hurricane Andrew can be detected using microseisms recorded at the Harvard, Massachusetts, seismic station even while the storm is as far as ~2000 km away and still at sea. When applied to decades of existing analog seismograms, this methodology could yield a seismically identified hurricane record for comparison to the pre-aircraft and pre-satellite observational record.

Introduction

Considerable uncertainty surrounds the question of whether anthropogenic global warming is changing the frequency or energy of hurricanes (Emanuel, 2005; Klotzbach, 2006; Holland and Webster, 2007; Knutson *et al.*, 2010), in part because it is unclear whether some or all of the apparent recent increases reflect the availability of data from aircraft and satellite observations (Landsea, 2007).

Because North Atlantic hurricane records before aircraft reconnaissance began in 1944 were based on storms making landfall in populated regions or chance encounters between hurricanes and ships at sea, hurricanes may have gone undetected (Neumann *et al.*, 1999; Fig. 1). Even after the initiation of regular aircraft observations, usually only western Atlantic weather systems were monitored. Potential sampling problems exist until the advent of satellite observation in the 1960s, making an undercount likely (Landsea, 2007).

One approach to this issue is to use storm-generated seismic signals (Peterson, 1993). Ambient seismic noise, also known as microseisms, is the pervasive background signal bathing the surface of Earth with energy at frequencies concentrated between 1000 and 50 mHz (periods between 1 and 20 s). The ambient seismic noise spectrum has two peaks: a primary but small one between ~83 and 56 mHz (periods of ~12–18 s) and a larger secondary one between ~250 and 110 mHz (periods of ~4–9 s). Secondary microseisms are generated at the seafloor by the coupling of atmospheric energy to oceanic gravity waves that generate pressure variations in the water column that do not decay with depth (Longuet-Higgins, 1950). The frequency of ocean swell resulting from storms depends on maximum storm wind speed (Bowen *et al.*, 2003) and generates microseismic energy at frequencies twice that of the swell.

That microseisms had a meteorological origin was recognized prior to Longuet-Higgins' theoretical explanation (Linke, 1909; Banerji, 1930; Gherzi, 1930; Gutenberg, 1931, 1936; Bradford, 1936). The link between microseisms and large storms was first verified experimentally in 1940 via an array of horizontal seismometers located near St. Louis, Missouri, which allowed rudimentary determination of wave velocity, source direction, and particle motion to be made (Ramirez, 1940a, b). Using data recorded by several three-element seismic arrays in the Caribbean region for more than 100 tropical storms and hurricanes between 1932 and 1944, Gilmore (1946) demonstrated a clear correlation between microseismic amplitudes and these energetic weather systems. Similar results were obtained in the western Pacific (Gilmore and Hubert, 1948). The use of microseisms in weather forecasting based on these results was discussed by Gutenberg (1947), but by the late 1940s the advantages promised by satellite-based observations discouraged weather-related research using microseisms.

The link between microseisms and storm energy has been a topic of recent investigation, with workers demonstrating that microseisms contain teleseismic body wave energy (Landès *et al.*, 2010; Zhang *et al.*, 2010) and examining microseisms generated by specific storms (Bromirski,

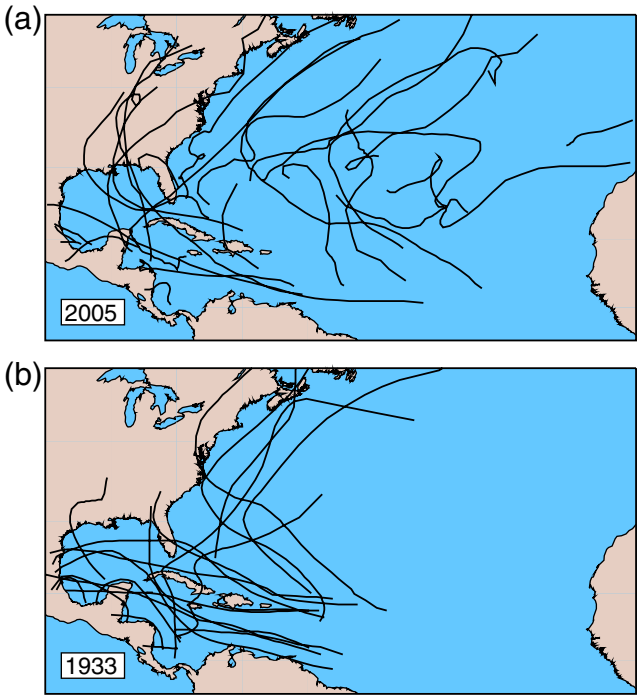

Figure 1. North Atlantic Ocean tracks for hurricanes, tropical storms, and depressions for two of the most active hurricane seasons: (a) 2005, gathered with the help of satellite observations, and (b) 1933, before aircraft reconnaissance began. (After Landsea, 2007). The color version of this figure is available only in the electronic edition.

2001; Gerstoft *et al.*, 2006). Because major storms increase microseismic energy (Astiz and Creager, 1994; Bromirski *et al.*, 1999; Grevemeyer *et al.*, 2000), ambient seismic noise has also been used to study climate variability on decadal scales (Aster *et al.*, 2008).

Data Analysis and Methodology

We explore the feasibility of developing methods to detect and characterize hurricanes to augment the existing pre-satellite era hurricane record. Our study uses data from the Harvard, Massachusetts, seismic station HRV, a long-lived high-quality installation in eastern North America near the path of North Atlantic hurricanes. Station HRV provides excellent records of microseisms generated by hurricanes because of low seismic wave attenuation in the old oceanic crust of the western Atlantic/Gulf of Mexico and the eastern United States craton (Canas and Mitchell, 1978; Okal and Talandier, 1989; Mitchell, 1995).

We base our methodology on power, which is proportional to the square of wave amplitude. Because we consider only relative changes in power, we do not remove seismometer response and use pseudopower, an arbitrary unit based on the square of the secondary microseism amplitude calculated using ground velocity data.

Hurricane Andrew

We focus on Hurricane Andrew, which took place in late August 1992 (Fig. 2). This Saffir/Simpson category 5 hurricane, one of the most powerful and destructive storms to hit the United States (Mayfield *et al.*, 1994; Landsea *et al.*, 2004), caused over $26 billion in direct losses (Rappaport, 1994) and 40 deaths (Longshore, 2008). The tropical depression that became Andrew was first monitored in the central North Atlantic on 16 August at 18:00 UTC (denoted as 16:18) and was upgraded the next day to a tropical storm. It was categorized as a hurricane at 6:00 UTC on 22 August and rapidly increased in intensity to category 5 (maximum wind speed greater than 249 km/hr or ~69 m/s) on 23 August. Andrew made landfall in the Bahamas on August 23:21 and at southeastern Florida at 9:00 UTC on 24 August. After crossing Florida and the Gulf of Mexico, Andrew made final landfall in Louisiana at 8:00 UTC on 26 August. Within two days Andrew was no longer monitored. Andrew is estimated to have reached category 5 intensity at landfall in both the Bahamas and southeastern Florida, and again by landfall in Louisiana.

Results

Figure 2a shows Andrew's maximum wind speed and pseudopower of secondary microseisms for August 1992 filtered in the 200 to 143 mHz (5 to 7 s) band and averaged over 6-hr segments. This signal reflects the distant hurricane rather than local storm activity, as shown both by weather maps from the National Oceanic and Atmospheric Administration (NOAA) and the relationship between maximum hurricane wind speed and microseism pseudopower. The initial rise in intensity while the storm is in the Atlantic is followed by a drop that begins when Andrew crosses shallow waters near the Bahamas and continues while the storm is over southern Florida and its western continental shelf. Both pseudopower and maximum wind speed then increase as Andrew intensifies again over the deeper waters of the Gulf of Mexico and decrease sharply after final landfall.

The distance between Andrew's eye and the HRV seismic station varies from ~1870 km on 22 August shortly after Andrew is first classified as a hurricane, to ~2310 km late on 25 August, about a half-day before final landfall. Because of attenuation, the amount of microseismic energy received at HRV is a function of Andrew-HRV distance. However, a distance correction is not applied because its effect would be secondary for this study: assuming typical values for microseism velocity and frequency, and a Q of 350 appropriate for Andrew-HRV paths (Canas and Mitchell, 1978; Okal and Talandier, 1989), amplitudes at HRV normalized to source amplitudes vary only between 0.38 and 0.46.

The microseism pseudopower and maximum wind speed correlate in detail, with a maximum correlation showing microseism energy lagging by about a half-day. The lag between the increase in maximum wind speed late on

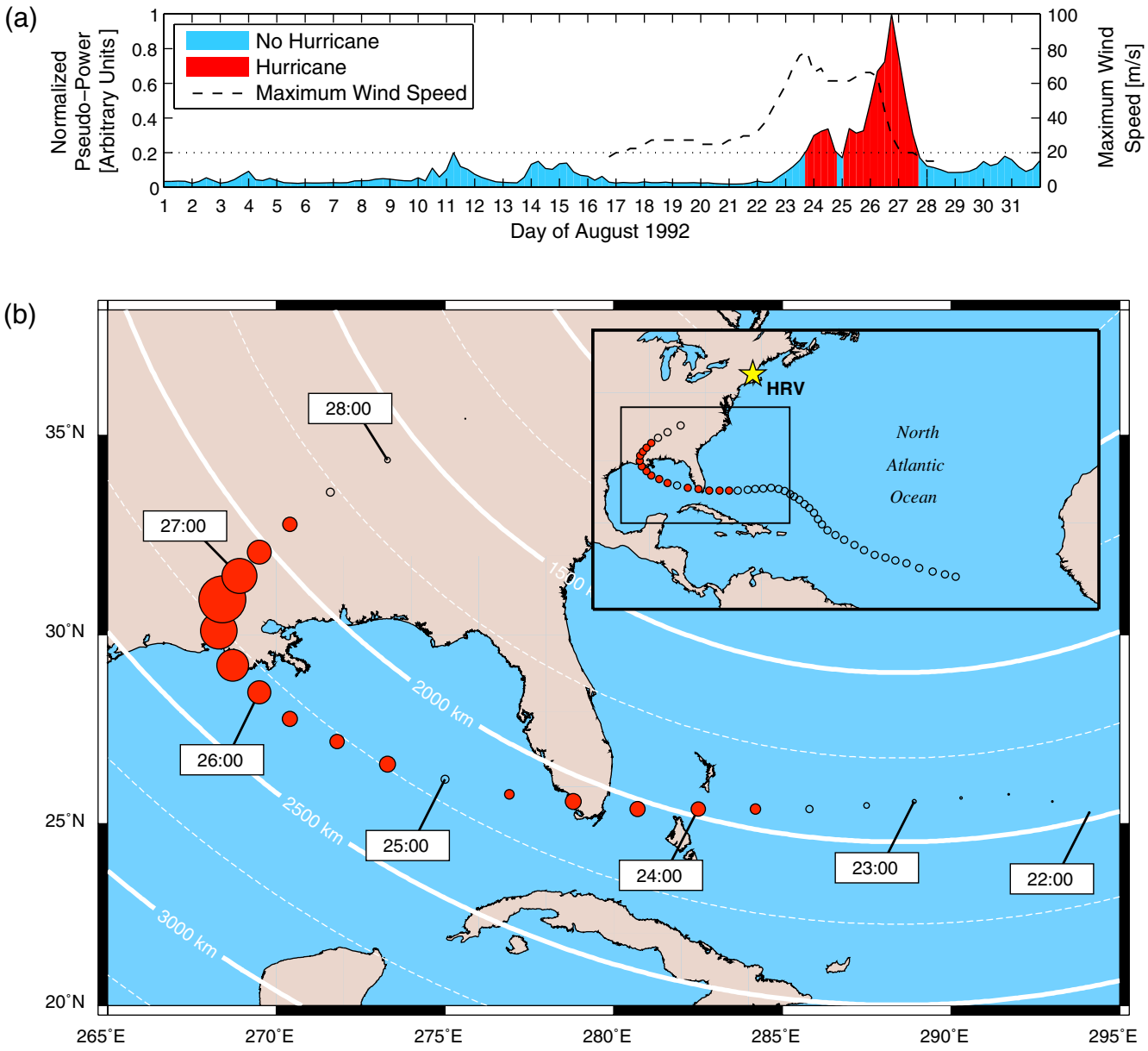

Figure 2. History of Hurricane Andrew shown by variation in microseism pseudopower at Harvard, Massachusetts, seismic station HRV. (a) Normalized time series band-pass-filtered between 200 and 143 mHz and smoothed using 6-hr means. Dotted line is empirical seismically identified hurricane (SIH) detection threshold. Maximum Andrew wind speed is shown with dashed line. Six-hour interval Andrew locations for the life of the storm are shown in the inset of (b), with the filled circles signifying storm locations at which the SIH threshold was exceeded. The large map shows 6-hr interval locations beginning at August 22:00, just before Andrew reached hurricane intensity, until August 28:06, after which time the storm was no longer monitored. Circle size is scaled to filtered microseism pseudopower amplitude. Andrew was identified seismically at location of filled circles. Contours at 250 km intervals show distance from HRV. The color version of this figure is available only in the electronic edition.

21 August and the rise in pseudopower around midday 22 August likely reflects the time needed for the development of wave conditions necessary to activate the Longuet-Higgins mechanism. The early 26 August drop in maximum wind speed precedes the decrease in pseudopower, presumably because the maximum wind speed is measured close to the storm's center whereas microseisms are generated over a broader area, especially in the portion of the hurricane trailing the eye (Longuet-Higgins, 1950). Figure 3 shows the normalized spectral amplitude of HRV microseism pseudopower for a 6-hr segment after final Andrew landfall late on 26 August, when pseudopower in the 200 to 143 mHz band was at its highest amplitude (Fig. 2). Thus, Andrew continued to generate microseisms for a significant amount of time after it made final landfall, as defined by the position of the eye.

Based on these results, we adopt a normalized microseism pseudopower amplitude of ~0.2 in the 200 to

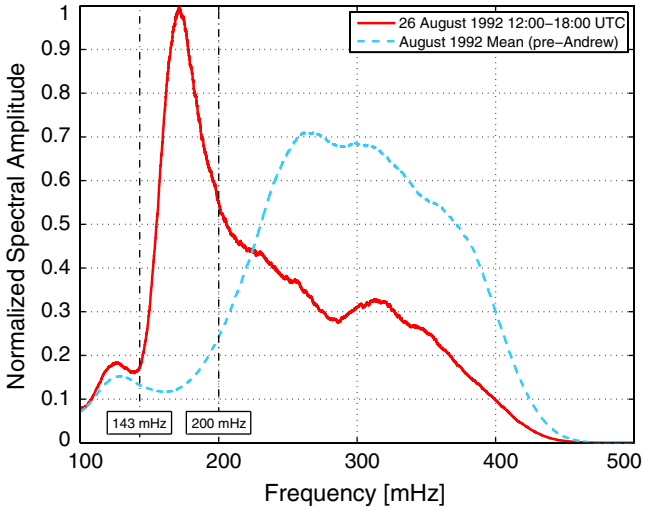

Figure 3. Summary of normalized HRV microseism pseudopower spectral amplitudes. The maximum amplitude in the 200 to 143 mHz passband occurs between 12:00 and 18:00 UTC on 26 August, shortly after Andrew made final landfall; the smoothed spectral amplitude curve for this segment is shown by the solid line. A smoothed mean spectral amplitude curve calculated from pre-Andrew 6-hr segments uncontaminated by earthquake arrivals is shown by the dashed line. Microseism pseudopower passband limits at 200 and 143 mHz are shown by dashed-dotted lines. The color version of this figure is available only in the electronic edition.

143 mHz passband to identify and characterize a seismically identified hurricane (SIH). Because Andrew was the only hurricane that formed during August 1992, we choose this threshold empirically to exclude all nonhurricane signals, such as those between 10 and 17 August (Fig. 2a).

Applying this SIH threshold, Andrew is first identified late on 23 August, about 36 hr after being designated a hurricane by NOAA. Hence, the hurricane can be identified seismically when it is ~1940 km from HRV and still at sea. Its pseudopower drops below the SIH threshold around midday August 27, about 18 hr after it lost NOAA hurricane status. Andrew is visible in the pseudopower signal as early as 12:00 UTC 22 August, when maximum wind speeds reach ~40 m/s. This is just 6 hr after the storm was first categorized as a hurricane, and about 24 hr before pseudopower amplitudes first exceed the SIH threshold.

Conclusions

This algorithm is successful in the posteriori detection of a powerful category 5 hurricane. The next steps are to investigate the suitability of a general detection threshold using microseismic signals generated by hurricanes and tropical storms with a range of intensities, and to explore whether the results can be extrapolated further to not only detect the existence of a hurricane and assess its intensity, but also to locate it. A detection threshold will likely be a function primarily of intensity, but because microseismic energy may be scattered at tectonic boundaries, a detection limit for storms, especially in the Caribbean region, is also likely to be a function of storm–seismic station travel paths. Beyond the scientific issues, a challenge in generating a record of seismically identified hurricanes lies with the effort required to digitize decades of analog seismograms.

Data and Resources

Seismic data used in this study can be obtained from the Incorporated Research Institutions for Seismology (IRIS) Data Management Center (DMC) (www.iris.edu; last accessed June 2010). Hurricane, depression, and storm track information and wind speed data were obtained from the National Oceanic and Atmospheric Administration (NOAA) Atlantic Oceanographic and Meteorological Laboratory, Hurricane Research Division Re-Analysis Project (www.aoml.noaa.gov/hrd/hurdat; last accessed October 2009). The Generic Mapping Tools software (www.soest.hawaii.edu/gmt) of Wessel and Smith (1991) was used to generate figures.

Acknowledgments

We thank the USGS Albuquerque Seismological Laboratory for the installation, maintenance, and operation of the HRV seismic station, part of the Global Seismic Network (GSN), and the IRIS DMC for data access. We thank BSSA associate editor Zhigang Peng and an anonymous reviewer for helpful comments. This work was supported by a National Science Foundation (NSF) Graduate Research Fellowship to CWE.

References

Aster, R., D. McNamara, and P. Bromirski (2008). Multidecadal climate-induced variability in microseisms, *Seismol. Res. Lett.* **79,** 194–202.

Astiz, L., and K. Creager (1994). Geographic and seasonal variations of microseismic noise, *Eos Trans. AGU* **75,** 419.

Banerji, S. (1930). Microseisms associated with disturbed weather in the Indian seas, *Phil. Trans. R. Soc. Lond. A* **229,** 287–328.

Bowen, S., J. Richard, J. Mancini, V. Fessatidis, and B. Crooker (2003). Microseism and infrasound generation by cyclones, *J. Acoust. Soc. Am.* **113,** 2562–2573.

Bradford, D. (1936). Microseisms and their relationship to changing meteorological conditions, *Bull. Seismol. Soc. Am.* **26,** 29–53.

Bromirski, P. (2001). Vibrations from the "perfect storm", *G³* **7,** doi 10.1029/2000GC000119.

Bromirski, P., R. Flick, and N. Graham (1999). Ocean wave height determined from inland seismometer data: Implications for investigating wave climate changes in the NE Pacific, *J. Geophys. Res.* **104,** 20753–20766.

Canas, J., and B. Mitchell (1978). Lateral variation of surface-wave anelastic attenuation across the Pacific, *Bull. Seismol. Soc. Am.* **68,** 1637–1650.

Emanuel, K. (2005). Increasing destructiveness of tropical cyclones over the past 30 years, *Nature* **49,** 349–353.

Gerstoft, P., M. Fehler, and K. Sabra (2006). When Katrina hit California, *Geophys. Res. Lett.* **33,** L17308, doi 10.1029/2006GL027270.

Gherzi, E. (1930). Microseisms associated with storms, *Gerlands Beiträge zur Geophysik* **25,** 145–147.

Gilmore, M. (1946). Microseisms and ocean storms, *Bull. Seismol. Soc. Am.* **36,** 89–119.

Gilmore, M., and W. Hubert (1948). Microseisms and Pacific typhoons, *Bull. Seismol. Soc. Am.* **38,** 195–228.

Grevemeyer, I., R. Herber, and H.-H. Essen (2000). Microseismological evidence for a changing wave climate in the northeast Atlantic Ocean, *Nature* **408,** 349–352.

Gutenberg, B. (1931). Microseisms in North America, *Bull. Seismol. Soc. Am.* **21,** 1–24.

Gutenberg, B. (1936). On microseisms, *Bull. Seismol. Soc. Am.* **26,** 111–117.

Gutenberg, B. (1947). Microseisms and weather forecasting, *J. Meteorol.* **4,** 21–28.

Holland, G., and P. Webster (2007). Heightened tropical cyclone activity in the North Atlantic: Natural variability or climate trend?, *Phil. Trans. R. Soc. A* **365,** 2695–2716.

Klotzbach, P. (2006). Trends in tropical cyclone activity over the past 20 years (1986–2005), *J. Geophys. Res.* **33,** L10805, doi 10.1029/2006GL025881.

Knutson, T., J. McBride, J. Chan, K. Emanuel, G. Holland, C. Landsea, I. Held, J. Kossin, A. Srivastava, and M. Sugi (2010). Tropical cyclones and climate change, *Nature Geosci.* doi 10.1038/NGEO779.

Landès, M., F. Hubans, N. Shapiro, A. Paul, and M. Campillo (2010). Origin of deep ocean microseisms by using teleseismic body waves, *J. Geophys. Res.* **115,** B05302, doi 10.1029/2009JB006918.

Landsea, C. (2007). Counting Atlantic tropical hurricanes back to 1900, *Eos Trans. AGU* **88,** 197–208.

Landsea, C., J. Franklin, C. McAdie, J. Beven II, J. Gross, B. Jarvinen, R. Pasch, E. Rappaport, J. Dunion, and P. Dodge (2004). A reanalysis of Andrew's intensity, *Bull. Am. Meteorol. Soc.* 1699–1712.

Linke, F. (1909). Die Brandungsbewegungen des Erdbodens und ein Versuch ihrer Verwendungen in der praktischen Meteorologie, *Abh. Ges. Wiss. Göttingen*, Neue Folge, 7 (in German).

Longshore, D. (2008). *Encyclopedia of Hurricanes, Typhoons, and Cyclones*, Checkmark Books, New York.

Longuet-Higgins, M. (1950). Theory of the origin of microseisms, *Phil. Trans. R. Soc. A* **243,** 1–35.

Mayfield, M., L. Avila, and E. Rappaport (1994). Annual summaries: Atlantic hurricane season of 1992, *Month. Weath. Rev.* **122,** 517–538.

Mitchell, B. (1995). Anelastic structure and evolution of the continental crust and upper mantle from seismic surface-wave attenuation, *Rev. of Geophys.* **33,** 441–462.

Neumann, C., B. Jarvinen, C. McAdie, and G. Hammer (1999). *Tropical Cyclones of the North Atlantic Ocean 1871–1998*, Tech. Rep., Natl. Oceanic and Atm. Admin., Asheville, North Carolina.

Okal, E., and J. Talandier (1989). M_m: A variable-period mantle magnitude, *J. Geophys. Res.* **94,** 4169–4204.

Peterson, J. (1993). Observations and modeling of seismic background noise, *U.S. Geol. Surv. Open-File Rept. 93-322*, Albuquerque, New Mexico.

Ramirez, J. (1940a). An experimental investigation of the nature and origin of microseisms at St. Louis, Missouri, Part One, *Bull. Seismol. Soc. Am.* **30,** 35–84.

Ramirez, J. (1940b). An experimental investigation of the nature and origin of microseisms at St. Louis, Missouri, Part Two, *Bull. Seismol. Soc. Am.* **30,** 139–178.

Rappaport, E. (1994). Hurricane Andrew, *Weather* **49,** 51–61.

Wessel, P., and W. Smith (1991). Free software helps map and display data, *Eos Trans. AGU* **72,** 441.

Zhang, J., P. Gerstof, and P. Shearer (2010). Resolving *P*-wave travel-time anomalies using seismic array observations of oceanic storms. *Earth Planet. Sci. Lett.* **292,** 419–427.

Department of Earth and Planetary Sciences
Northwestern University
1850 Campus Drive
Evanston, Illinois 60208
carl@earth.northwestern.edu

Manuscript received 21 June 2010